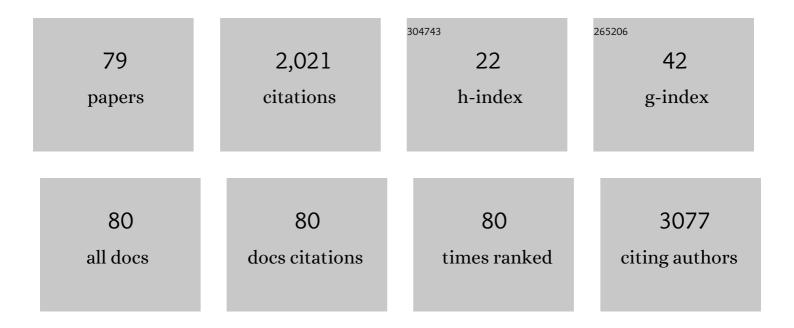
## Ji-Won Choi

List of Publications by Year in descending order

Source: https://exaly.com/author-pdf/6081063/publications.pdf Version: 2024-02-01



#	Article	IF	CITATIONS
1	Issue and challenges facing rechargeable thin film lithium batteries. Materials Research Bulletin, 2008, 43, 1913-1942.	5.2	514
2	Recent Advances in the Nanocatalyst-Assisted NaBH <sub>4</sub> Reduction of Nitroaromatics in Water. ACS Omega, 2019, 4, 483-495.	3.5	180
3	Copper oxide–graphene oxide nanocomposite: efficient catalyst for hydrogenation of nitroaromatics in water. Nano Convergence, 2019, 6, 6.	12.1	94
4	Synthesis of SnS Thin Films by Atomic Layer Deposition at Low Temperatures. Chemistry of Materials, 2017, 29, 8100-8110.	6.7	68
5	Recent Advances in Rechargeable Aluminum-Ion Batteries and Considerations for Their Future Progress. ACS Applied Energy Materials, 2020, 3, 6019-6035.	5.1	58
6	+Iron hexacyanocobaltate metal-organic framework: Highly reversible and stationary electrode material with rich borders for lithium-ion batteries. Journal of Alloys and Compounds, 2019, 791, 911-917.	5.5	54
7	Scalable fabrication of flexible thin-film batteries for smart lens applications. Nano Energy, 2018, 53, 225-231.	16.0	53
8	Two-dimensional boron nitride as a sulfur fixer for high performance rechargeable aluminum-sulfur batteries. Scientific Reports, 2019, 9, 13573.	3.3	44
9	Superior Additive of Exfoliated RuO <sub>2</sub> Nanosheet for Optimizing the Electrode Performance of Metal Oxide over Graphene. Journal of Physical Chemistry C, 2016, 120, 11786-11796.	3.1	40
10	Full range optical and electrical properties of Zn-doped SnO2 and oxide/metal/oxide multilayer thin films deposited on flexible PET substrate. Journal of Alloys and Compounds, 2017, 694, 217-222.	5.5	40
11	Laser-irradiated inclined metal nanocolumns for selective, scalable, and room-temperature synthesis of plasmonic isotropic nanospheres. Journal of Materials Chemistry C, 2018, 6, 6038-6045.	5.5	37
12	Properties of CoS2/CNT as a Cathode Material of Rechargeable Aluminum-Ion Batteries. Electronic Materials Letters, 2019, 15, 727-732.	2.2	33
13	Layered metal–organic framework based on tetracyanonickelate as a cathode material for <i>in situ</i> Li-ion storage. RSC Advances, 2019, 9, 21363-21370.	3.6	32
14	Low-temperature wafer-scale synthesis of two-dimensional SnS <sub>2</sub> . Nanoscale, 2018, 10, 17712-17721.	5.6	30
15	Carbon-free Mn-doped LiFePO4 cathode for highly transparent thin-film batteries. Journal of Power Sources, 2019, 434, 226713.	7.8	29
16	Realization of Lithium-Ion Capacitors with Enhanced Energy Density via the Use of Gadolinium Hexacyanocobaltate as a Cathode Material. ACS Applied Materials & Interfaces, 2019, 11, 31799-31805.	8.0	28
17	Coordinating gallium hexacyanocobaltate: Prussian blue-based nanomaterial for Li-ion storage. RSC Advances, 2019, 9, 26668-26675.	3.6	28
18	Metal-organic framework-derived metal oxide nanoparticles@reduced graphene oxide composites as cathode materials for rechargeable aluminium-ion batteries. Scientific Reports, 2019, 9, 13739.	3.3	28

JI-WON CHOI

#	Article	IF	CITATIONS
19	A Hybrid Energy Storage Mechanism of Zinc Hexacyanocobaltate-Based Metal–Organic Framework Endowing Stationary and High-Performance Lithium-Ion Storage. Electronic Materials Letters, 2019, 15, 444-453.	2.2	28
20	Formation of high concentrations of isolated Zn vacancies and evidence for their acceptor levels in ZnO. Journal of Alloys and Compounds, 2017, 729, 1031-1037.	5.5	24
21	Enhancement of Mechanical Hardness in SnO <sub><i>x</i></sub> N <sub><i>y</i></sub> with a Dense High-Pressure Cubic Phase of SnO <sub>2</sub> . Chemistry of Materials, 2016, 28, 7051-7057.	6.7	23
22	S@GO as a High-Performance Cathode Material for Rechargeable Aluminum-Ion Batteries. Electronic Materials Letters, 2019, 15, 720-726.	2.2	23
23	Graphite carbon-encapsulated metal nanoparticles derived from Prussian blue analogs growing on natural loofa as cathode materials for rechargeable aluminum-ion batteries. Scientific Reports, 2019, 9, 13665.	3.3	23
24	Cerium Hexacyanocobaltate: A Lanthanide-Compliant Prussian Blue Analogue for Li-Ion Storage. ACS Omega, 2019, 4, 21410-21416.	3.5	23
25	Tailorable Topologies for Selectively Controlling Crystals of Expanded Prussian Blue Analogues. Crystal Growth and Design, 2019, 19, 7385-7395.	3.0	21
26	Wafer-Scale, Conformal, and Low-Temperature Synthesis of Layered Tin Disulfides for Emerging Nonplanar and Flexible Electronics. ACS Applied Materials & Interfaces, 2020, 12, 2679-2686.	8.0	20
27	Crystal structure and piezoelectric characteristics of various phases near the triple-point composition in PZ-PT-PNN system. Journal of the European Ceramic Society, 2020, 40, 1947-1956.	5.7	19
28	Electrical and optical properties of Ga doped zinc oxide thin films deposited at room temperature by continuous composition spread. Applied Surface Science, 2010, 256, 6219-6223.	6.1	18
29	Electrophoretic deposition of Ca <sub>2</sub> Nb <sub>3</sub> O <sub>10</sub> <sup>â^'</sup> nanosheets synthesized by soft-chemical exfoliation. Journal of Materials Chemistry C, 2016, 4, 178-184.	5.5	18
30	Thermally stable high strain and piezoelectric characteristics of (Li, Na, K)(Nb,) Tj ETQq0 0 0 rgBT /Overlock 10 Tf Society, 2019, 102, 6115-6125.	50 307 To 3.8	l (Sb)O <sub 18</sub 
31	Electrochemical properties of Li[Li0.2Mn0.54Co0.13Ni0.13]O2 cathode thin film by RF sputtering for all-solid-state lithium battery. Journal of Solid State Chemistry, 2012, 196, 288-292.	2.9	17
32	Doped SnO <sub>2</sub> Transparent Conductive Multilayer Thin Films Explored by Continuous Composition Spread. ACS Combinatorial Science, 2015, 17, 247-252.	3.8	17
33	Electrochemical activity of Samarium on starch-derived porous carbon: rechargeable Li- and Al-ion batteries. Nano Convergence, 2020, 7, 11.	12.1	16
34	Influence of substrate temperature on the electrical and optical properties of Ga-doped ZnO thin films fabricated by continuous composition spread. Ceramics International, 2012, 38, S605-S608.	4.8	15
35	Full Range Dielectric Characteristics of Calcium Copper Titanate Thin Films Prepared by Continuous Composition-Spread Sputtering. ACS Combinatorial Science, 2014, 16, 478-484.	3.8	15
36	Highly conductive and damp heat stable transparent ZnO based thin films for flexible electronics. Journal of Alloys and Compounds, 2013, 554, 240-245.	5.5	14

JI-WON CHOI

#	Article	IF	CITATIONS
37	Synthesis of Sr <sub>2</sub> Nb <sub>3</sub> O <sub>10</sub> nanosheets and their application for growth of thin film using an electrophoretic method. Journal of the American Ceramic Society, 2017, 100, 1098-1107.	3.8	14
38	Various cubic-based polymorphic phase boundary structures in (1-y)(Na0.5K0.5)(Nb1-xSbx)-yCaTiO3 ceramics and their piezoelectric properties. Journal of the European Ceramic Society, 2019, 39, 973-985.	5.7	14
39	Rapid Defrost Transparent Thin-Film Heater with Flexibility and Chemical Stability. ACS Applied Materials & Interfaces, 2020, 12, 38406-38414.	8.0	12
40	Phase evolution and Sn-substitution in LiMn2O4 thin films prepared by pulsed laser deposition. Journal of Electroceramics, 2009, 23, 200-205.	2.0	11
41	Essential Macleod Program (EMP) simulated fabrication of high quality Zn:SnO 2 /Ag/Zn:SnO 2 multilayer transparent conducting electrode on flexible substrates. Ceramics International, 2017, 43, 7216-7221.	4.8	11
42	Performance enhancement in organic photovoltaic solar cells using iridium (Ir) ultra-thin surface modifier (USM). Applied Surface Science, 2018, 444, 97-104.	6.1	11
43	Zn Vacancy Formation Energy and Diffusion Coefficient of CVT ZnO Crystals in the Sub-Surface Micron Region. Scientific Reports, 2018, 8, 13446.	3.3	11
44	Hybrid Thin-Film Encapsulation for All-Solid-State Thin-Film Batteries. ACS Applied Materials & Interfaces, 2020, 12, 11504-11510.	8.0	11
45	Giant Electroresistive Ferroelectric Diode on 2DEG. Scientific Reports, 2015, 5, 10548.	3.3	10
46	Critical increase in Na-doping facilitates acceptor band movements that yields ~180 meV shallow hole conduction in ZnO bulk crystals. Scientific Reports, 2017, 7, 44196.	3.3	10
47	Correlation Between Temperature Coefficient of Resonant Frequency and Tetragonality Ratio. Journal of the American Ceramic Society, 2006, 89, 1144-1146.	3.8	9
48	Synthesis and piezoelectric properties of (1 â^' x)(Na0.5K0.5)NbO3–x(Ba0.95Sr0.05)TiO3 ceramics. Journal of Electroceramics, 2009, 23, 502-505.	2.0	9
49	Photoluminescence studies on MBE grown Co-doped ZnO thin films fabricated through ion implantation and swift heavy ion irradiation. Nuclear Instruments & Methods in Physics Research B, 2012, 272, 305-308.	1.4	9
50	Dielectric properties of single crystal Sr 2 Nb 3 O 10 dielectric nanosheet thin films by electrophoretic deposition (EPD) and post deposition treatments. Journal of Alloys and Compounds, 2017, 711, 51-57.	5.5	9
51	3D architectures of single-crystalline complex oxides. Materials Horizons, 2020, 7, 1552-1557.	12.2	9
52	Silver alloy-based metal matrix composites: a potential material for reliable transparent thin film heaters. Journal of Materials Chemistry C, 2021, 9, 4670-4681.	5.5	9
53	Rendering Redox Reactions of Cathodes in Li-Ion Capacitors Enabled by Lanthanides. ACS Omega, 2020, 5, 1634-1639.	3.5	9
54	Microwave dielectric properties of Ca[(Li1/3Nb2/3)1â^'x Tix]O3â^´Î´ ceramics with glass. Journal of Electroceramics, 2006, 17, 399-403.	2.0	8

#	Article	IF	CITATIONS
55	Defect-Controlled, Scalable Layer-by-Layer Assembly of High-k Perovskite Oxide Nanosheets for All Two-Dimensional Nanoelectronics. Chemistry of Materials, 2021, 33, 8685-8692.	6.7	8
56	Optical Properties and Electrochemical Performance of LiFePO <sub>4</sub> Thin Films Deposited on Transparent Current Collectors. Journal of Nanoscience and Nanotechnology, 2015, 15, 8627-8631.	0.9	7
57	High work function MoO 2 and ReO 2 contacts for p -type Si and GaN by a room-temperature non-vacuum process. Materials Science in Semiconductor Processing, 2017, 71, 374-377.	4.0	7
58	Dielectric and patch antenna characteristics of new high-Q (1 â^ x)(Al1/2Ta1/2)O2â^ x(Mg1/3Ta2/3)O2 (0 ≤)	Tj ETQq0 4.0	0 g rgBT /Ov
59	Synthesis and dielectric properties of HCa2Nb3O10 layered structure ceramics. Ceramics International, 2013, 39, S611-S614.	4.8	6
60	A novel class of oxynitrides stabilized by nitrogen dimer formation. Scientific Reports, 2018, 8, 14471.	3.3	6
61	Synthesis of large monolayer titania nanosheets through flux method. Journal of Asian Ceramic Societies, 2021, 9, 916-925.	2.3	6
62	Synthesis and dielectric properties of strontium substituted calcium niobate ceramics. Journal of Alloys and Compounds, 2015, 622, 373-378.	5.5	5
63	Sr2Nb3O10 nanosheet thin film grown via LB method for high-performance planar-type pseudocapacitor. Applied Surface Science, 2020, 525, 146640.	6.1	5
64	Transparent SiN thin-film anode for thin-film batteries by reactive sputtering at room temperature. Chemical Engineering Journal, 2020, 401, 126086.	12.7	5
65	Highly Transparent MTO/Ag/MTO Multilayer Film Deposited on Polyethylene Terephthalate Substrate for Transparent Conductive Oxide. Journal of Nanoscience and Nanotechnology, 2017, 17, 7218-7222.	0.9	5
66	LiMn2O4-based cathode thin films for Li thin-film batteries. Journal of the Korean Physical Society, 2016, 68, 41-53.	0.7	4
67	Exploration of Si-doped SnO2 composition and properties of oxide/Ag/oxide multilayers prepared using continuous composition spread by sputtering. Thin Solid Films, 2018, 660, 606-612.	1.8	4
68	Dielectric properties of composition spread SiO2–Al2O3 mixed phase thin films deposited at room temperature by off-axis RF magnetron sputtering. Ceramics International, 2012, 38, S79-S82.	4.8	3
69	Piezoelectric properties of highly densified 0.01Pb (Mg1/2W1/2)O3–0.41Pb (Ni1/3Nb2/3)O3–0.35PbTiO3–0.23PbZrO3+0.1 wt% Y2O3+1.5 wt% ZnO thick films on alumina substrate. Ceramics International, 2013, 39, 1327-1333.	4.8	3
70	Sn-substituted LiMn2O4 thin films prepared by RF magnetron sputtering. Solid State Sciences, 2013, 16, 13-15.	3.2	3
71	Improved piezoelectric properties of lead-free (1â^'x)(Na0.5K0.5)NbO3–x(Ba0.95Sr0.05)TiO3 ceramics by particle size control. Ceramics International, 2014, 40, 12023-12028.	4.8	3
72	Continuous Composition Spread and Electrochemical Studies of Low Cobalt Content Li(Ni,Mn,Co)O2 Cathode Materials. Coatings, 2019, 9, 366.	2.6	3

JI-WON CHOI

#	Article	IF	CITATIONS
73	Effect of the Octahedral Bond Valence on Microwave Dielectric Properties of (1-x)Al0.5Ta0.5O2-xMg0.33Ta0.67O2 Ceramics. Journal of the American Ceramic Society, 2006, 89, 1083-1086.	3.8	1
74	Dielectric properties of continuous composition spreaded MgO–Ta2O5 thin films. Applied Surface Science, 2011, 258, 843-847.	6.1	1
75	Atomic Doping Site and Dielectric Property in Perovskite Oxide Nanosheets. Microscopy and Microanalysis, 2019, 25, 2152-2153.	0.4	1
76	Design of dispersion-free dielectrics as engineering perovskite unit cells of KCa2Li(n-3)NbnO3n+1 ceramics. Ceramics International, 2021, 47, 17331-17336.	4.8	1
77	Structural characteristics of new high-Q (1â^'x)(Al1/2Ta1/2)O2–x(Mg1/3Ta2/3)O2 (0.2 <x<1.0) 2003,="" 243-246.<="" 79,="" and="" ceramics.="" chemistry="" materials="" microwave="" physics,="" td=""><td>4.0</td><td>0</td></x<1.0)>	4.0	0
78	Role of Alumina Buffer Layer on the Dielectric and Piezoelectric Properties of PZT System Thick Films. Journal of the American Ceramic Society, 2013, 96, 491-495.	3.8	0
79	Micro batteries for driving glucose sensors on smart lenses. , 2016, , .		Ο